

Association of compromised cerebral perfusion with lenticulostriate artery impairments in the subacute phase of branch atheromatous disease

Shuai Jiang , Jing-Yu Cui, Yu-Ying Yan, Tang Yang, Wen-Dan Tao and Bo Wu

Ther Adv Neurol Disord

2022, Vol. 15: 1–13

DOI: 10.1177/
17562864221109746

© The Author(s), 2022.
Article reuse guidelines:
[sagepub.com/journals-](https://sagepub.com/journals-permissions)
permissions

Abstract

Background Purpose: Whether altered cerebral perfusion is associated with the pathogenesis of single subcortical infarctions (SSIs) in the lenticulostriate artery (LSA) territory remains unclear.

Objective: We aimed to assess whether cerebral perfusion abnormalities are related to LSA impairments in the subacute phase of SSIs and then to examine their correlations with etiological subtypes of SSIs.

Methods: A total of 110 patients with acute SSIs in the LSA territory were prospectively recruited between July 2017 and October 2021, and they underwent magnetic resonance perfusion-weighted imaging (PWI) and whole-brain vessel-wall imaging (VWI) within 7 days of stroke onset. Based on VWI, patients were assigned to one of two SSI subtypes: branch atheromatous disease (BAD, $n = 78$, 70.9%) or lacunar infarction related to cerebral small vessel disease (CSVD-related LI, $n = 32$, 29.1%). Perfusion maps and LSA morphology were also quantitatively assessed.

Results: Based on PWI, 22 patients (20%) had hypoperfusion and 88 (80%) showed normal perfusion. Compared with normal individuals, patients with hypoperfusion showed shorter average LSA length (23.48 ± 4.81 mm versus 25.47 ± 3.74 mm, $p = 0.037$). Compared with patients with CSVD-related LI, patients with BAD had significantly lower relative cerebral blood flow [0.95 (IQR 0.81 – 1.12) versus 1.04 (IQR 0.92 – 1.22); $p = 0.036$] and cerebral blood volume [0.95 (IQR 0.84 – 1.15) versus 1.14 (IQR 0.97 – 1.27); $p = 0.020$] after adjusting for hypertension, number of LSA branches, and infarct volume.

Conclusion: Compromised cerebral perfusion is associated with impairments in the LSA and with BAD pathogenesis. Perfusion magnetic resonance imaging can provide important insights into acute SSI pathophysiology, and it may be useful for determining the clinical significance of perfusion abnormalities in BAD occurrence.

Keywords: branch atheromatous disease, cerebral small vessel disease, lenticulostriate artery, perfusion-weighted imaging, vessel-wall imaging

Received: 11 May 2022; revised manuscript accepted: 9 June 2022.

Introduction

Single subcortical infarctions (SSIs) in the lenticulostriate artery (LSA) territory without stenotic middle cerebral artery are heterogeneous conditions. Lipohyalinosis and branch atheromatous disease (BAD) were two main types of underlying vascular pathology based on the meticulous postmortem

work of Fisher and Caplan.^{1–3} Lipohyalinosis is commonly considered to be representative of intrinsic cerebral small vessel disease (CSVD), traditionally called ‘lacunar infarction’ (defined as CSVD-related LI). BAD is caused by occlusion or stenosis of perforating vessels due to microatheromas or junctional plaques.³ Whether and how

Correspondence to:

Bo Wu
Department of Neurology,
West China Hospital,
Sichuan University, No. 37,
Guo Xue Xiang, Chengdu
610041, Sichuan, China
dr.bowu@hotmail.com

Shuai Jiang
Jing-Yu Cui
Yu-Ying Yan
Tang Yang
Wen-Dan Tao
Department of Neurology,
West China Hospital,
Sichuan University,
Chengdu, China

CSVD-related LI and BAD contribute to the pathogenesis of SSIs is unclear, as the small size of the brain and vascular lesions hinders *in vivo* imaging of LSAs.

Magnetic resonance perfusion-weighted imaging (PWI) can detect perfusion deficits in patients with SSIs despite their small volume,⁴⁻¹⁰ and whole-brain vessel-wall imaging (VWI) can visualize LSAs.¹¹⁻¹³ These tools therefore provide a basis for exploring SSI pathogenesis. Our group, for example, simultaneously visualized the spatial relationship between the middle cerebral artery plaque and the LSA origin, allowing us to detect a smaller number of LSA branches in patients with BAD than in patients with CSVD-related LI.¹³ This result suggests heterogeneous pathogenesis of SSIs.

Whether the observed alterations in LSA morphology reflect alterations in cerebral perfusion is unclear. Therefore, in the present study, we used our recently established VWI-based etiological classification of SSIs¹³ to assess whether abnormal cerebral perfusion is related to impairments in the LSA in patients with acute SSIs.

Methods

Patients

We reviewed data from the prospectively collected acute SSIs database of the Department of Neurology at West China Hospital between July 2017 and October 2021. Patients were included if they (1) had a first-ever SSI in the unilateral LSA territory (basal ganglia, corona radiata, and internal capsule) confirmed by diffusion-weighted imaging (DWI); (2) underwent magnetic resonance PWI and VWI within 7 days of the onset of symptoms; and (3) had no stenosis of the relevant middle cerebral artery on magnetic resonance angiography (MRA).

Patients were excluded if they (1) had $\geq 50\%$ stenosis of the ipsilateral internal carotid artery, as determined by computed tomography angiography or MRA; (2) had non-atherosclerotic vasculopathies, such as dissection, vasculitis, or moyamoya disease; or (3) received thrombolytic therapy after symptom onset. Patients were also excluded if (4) transthoracic echocardiography and 24-h electrocardiographic or Holter monitoring identified high-risk

factors for cardioembolism, such as atrial fibrillation, valvular heart disease, infective endocarditis, and patent foramen ovale; or (5) image quality was inadequate for quantitative analysis.

Data collection

Data were collected on demographic features and risk factors including age, sex, blood pressure on admission, current smoking status, and medical history of hypertension, diabetes mellitus, hyperlipidemia, coronary artery disease, atrial fibrillation, and cerebrovascular disease. Baseline neurological deficits were assessed using the National Institutes of Health Stroke Scale (NIHSS). Early neurological deterioration (END) was defined as an elevation in the total NIHSS score ≥ 2 or an increase in NIHSS score ≥ 1 in the motor item within 7 days of stroke onset. Functional outcome at 90 days was determined by trained stroke neurologists using the modified Rankin Scale (mRS). Poor outcome was defined as an mRS ≥ 2 at 90 days.

Magnetic resonance imaging

Magnetic resonance imaging (MRI) examinations, including conventional T1-weighted, T2-weighted, fluid-attenuated inversion recovery imaging, DWI, 3D time-of-flight MRA, whole-brain VWI, and dynamic susceptibility contrast-PWI, were performed on a research-dedicated 3-Tesla Siemens Trio MRI system (Siemens Medical Systems, Erlangen, Germany) with a 32-channel head coil. PWI scans were obtained using a gradient-echo echo-planar imaging sequence. After a bolus injection of 0.2 mmol/kg of a gadolinium-based contrast agent (Magnevist; Schering, Berlin, Germany) into the antecubital vein (injection speed, 4 ml/s), perfusion images were acquired with the following parameters: repetition time, 1500 ms; echo time, 32 ms; flip, 90; field-of-view, 220 \times 220 mm; matrix size, 128 \times 128. A total of 19 slices with a thickness of 5 mm and a slice gap of 1.5 mm were then obtained and imaged at 50 frames/slice with a total imaging time of 83 s. The detailed imaging parameters of other sequences can be found in our previous studies.^{12,13}

Image analysis

All images were reviewed and analyzed by two experienced investigators (S.J. and J.-Y.C.) blinded to the clinical data. VWI readers were

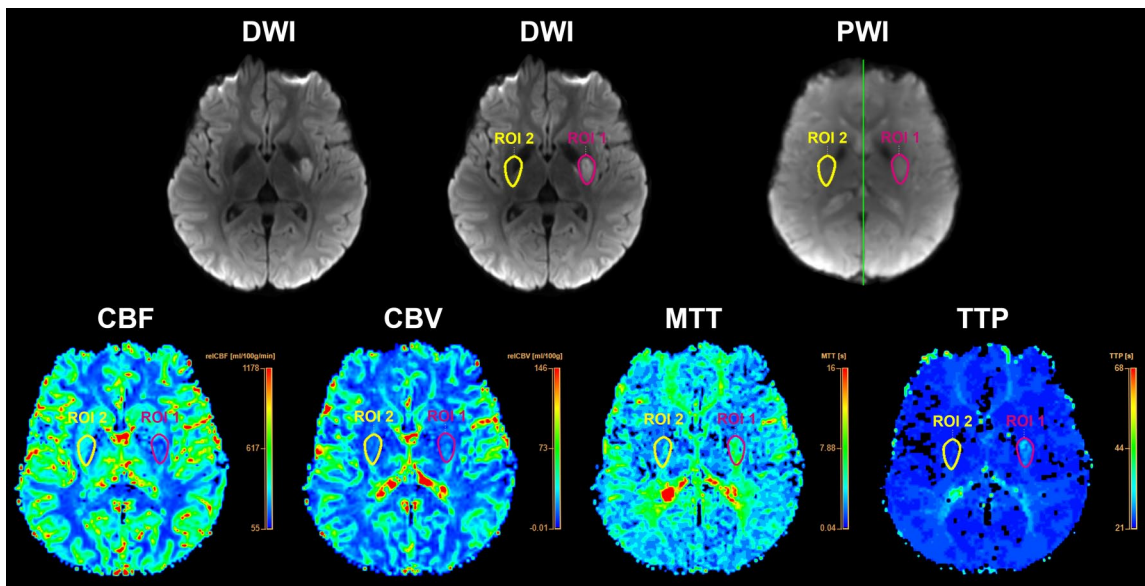


Figure 1. Co-registration of imaging and definition of regions of interest (ROIs). An ROI was defined on the acute infarction in the DWI map (ROI 1) and mirrored to the contralateral unaffected hemisphere (ROI 2). Then, each ROI was automatically co-registered onto the perfusion maps of cerebral blood flow (CBF), cerebral blood volume (CBV), mean transit time (MTT), and time to peak (TTP). The relative CBF, CBV, MTT, and TTP values of the infarct lesion were calculated as the ratio of ROI 1 to ROI 2. The green line represents the midline.

blinded to perfusion assessment. In the case of discrepancies, the images were reviewed again by both readers and discussed until consensus was reached. Inter-observer agreement on quantitative perfusion parameters were assessed in terms of the intraclass correlation coefficient (95% confidence interval), which was 0.88 (0.73–0.96) for relative cerebral blood flow (rCBF), 0.87 (0.67–0.95) for relative cerebral blood volume (rCBV), 0.95 (0.86–0.98) for relative mean transit time (rMTT), and 0.83 (0.54–0.94) for relative time to peak (rTTP). The inter-observer reliability for the evaluation of LSA morphology was also excellent based on our previous findings.¹²

PWI post-processing

Raw PWI images were processed using the IntelliSpace Portal (version 9.05, Philips Healthcare, Netherlands) and the MRI Neuro Perfusion package with the manual arterial input function. Perfusion maps of CBF, CBV, MTT, and TTP were generated using a delay-insensitive deconvolution technique. To overcome the inherent limitations of visual inspection, we used an image-processing pipeline to quantitatively detect perfusion defects in perfusion maps.

First, DWI images were co-registered to the parametric maps. Based on visual inspection, a region of interest (ROI) was manually outlined, slice by slice, to cover the hyperintense area of SSI in the DWI map (ROI 1) and was mirrored to the contralateral unaffected hemisphere (ROI 2). After automatic co-registration into the perfusion maps, the respective voxel-wise mean CBF, CBV, MTT, and TTP values were calculated (Figure 1). Next, the final voxel-wise mean perfusion values representing the weighted average value of each ROI were calculated based on a previous method.¹⁴ Normalized rCBF, rCBV, rMTT, and rTTP values were calculated as the ratio of ROI 1 to ROI 2.

Hypoperfusion and normal perfusion

Since there are no validated or consensus absolute perfusion values for differentiating tissues at risk from benign oligemic tissues,¹⁵ we identified the regions with detectably reduced cerebral perfusion by applying a relative perfusion threshold of 75% (25% perfusion reduction) based on a previous study.¹⁰ The identified regions were then classified as showing hypoperfusion or normal perfusion. Hypoperfusion was defined as a

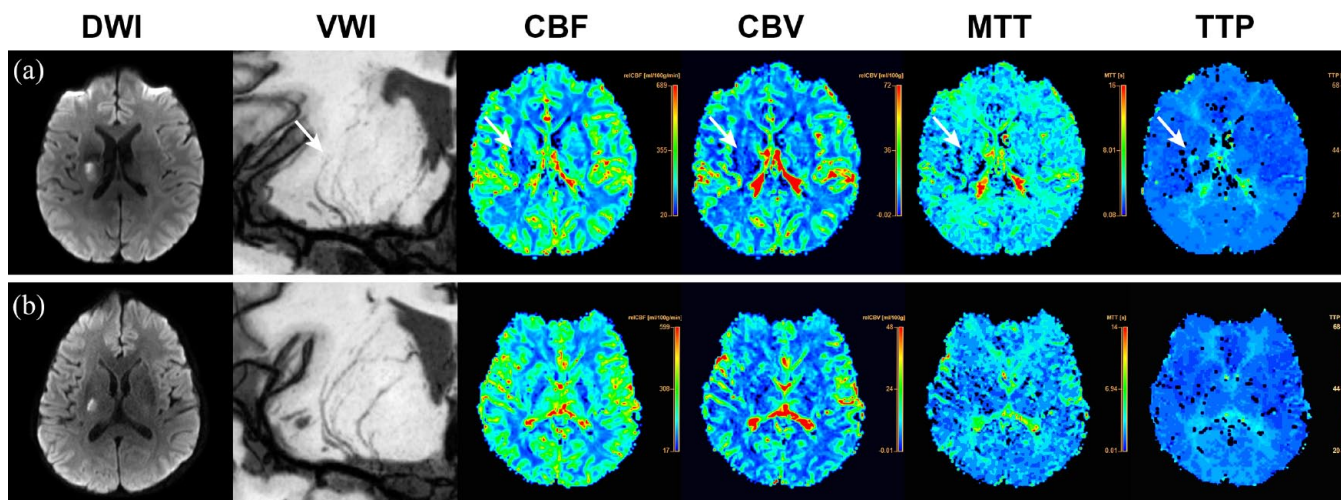


Figure 2. Two representative examples of the perfusion patterns. (a) Hypoperfusion: acute single subcortical infarction (SSI) in the right basal ganglia on diffusion-weighted imaging (DWI) with reduced cerebral blood flow (CBF) and cerebral blood volume (CBV), and prolonged mean transit time (MTT) and time to peak (TTP) (white arrows). The reconstructed coronal minimum-intensity projection (MinIP) of vessel-wall magnetic resonance imaging (VWI) showed shorter lengths of the right lenticulostriate arteries (white arrow). (b) Normal perfusion: acute SSI in the right basal ganglia on DWI without perfusion defects. The coronal MinIP of VWI revealed almost normal lenticulostriate arteries in the ipsilateral right hemisphere.

decrease in rCBF and rCBV or an increase in rMTT and rTTP differing more than 25% from the values in the contralateral hemisphere. Normal perfusion was defined as a decrease in rCBF and rCBV or increase in rMTT and rTTP within 25% of the values in the contralateral hemisphere (Figure 2).

MRI analysis

Acute SSIs in the LSA territory were diagnosed according to an existing template¹⁶ identified by DWI. The maximal diameter of 20mm was not used as a cutoff, as it remains unclear whether the lesion diameter is an appropriate criterion for classifying stroke subtypes.¹⁷ The infarct volume was measured using DWI by manually delineating ROI slices, and the total volume for all ROIs was calculated using commercial software (OsiriX MD, Pixmeo SARL, Bernex, Switzerland).

Analysis of the LSA and classification of BAD and CSVD-related LI by VWI

The morphology of LSAs was quantitatively assessed using OsiriX MD software. For simultaneous visualization of the middle cerebral artery lumen and LSA morphology, multi-planar reconstruction (MPR) and coronal minimum-intensity

projection (MinIP) were generated in one image setting with VWI images. The LSA skeleton was delineated by manually tracing the central lines of the arteries, and the morphological characteristics of visible LSAs (number of stems and branches, length, distance, and tortuosity) were quantitatively analyzed on the consecutive coronal slab MinIP images. The full vessel length was defined as the actual path length between the origin and the terminal of an LSA, while the vessel distance was defined as the linear distance between the two endpoints of an LSA. LSA tortuosity was calculated by dividing the actual path length by the linear distance. The etiological subtypes of SSIs were classified based on VWI as either BAD, when a culprit plaque was adjacent to the LSA origin (Figure 3(a)); or as CSVD-related LI, when the plaque was absent or located far from the LSA origin (Figure 3(b)). More detailed explanations of LSA morphometry and SSI classification have been published elsewhere.^{12,13}

Statistical analysis

Statistical analyses were performed with the Statistical Package for the Social Sciences (SPSS) statistical software (version 25.0, Chicago, IL, USA). The normal distribution of all variables was assessed using the Shapiro–Wilk test. Quantitative

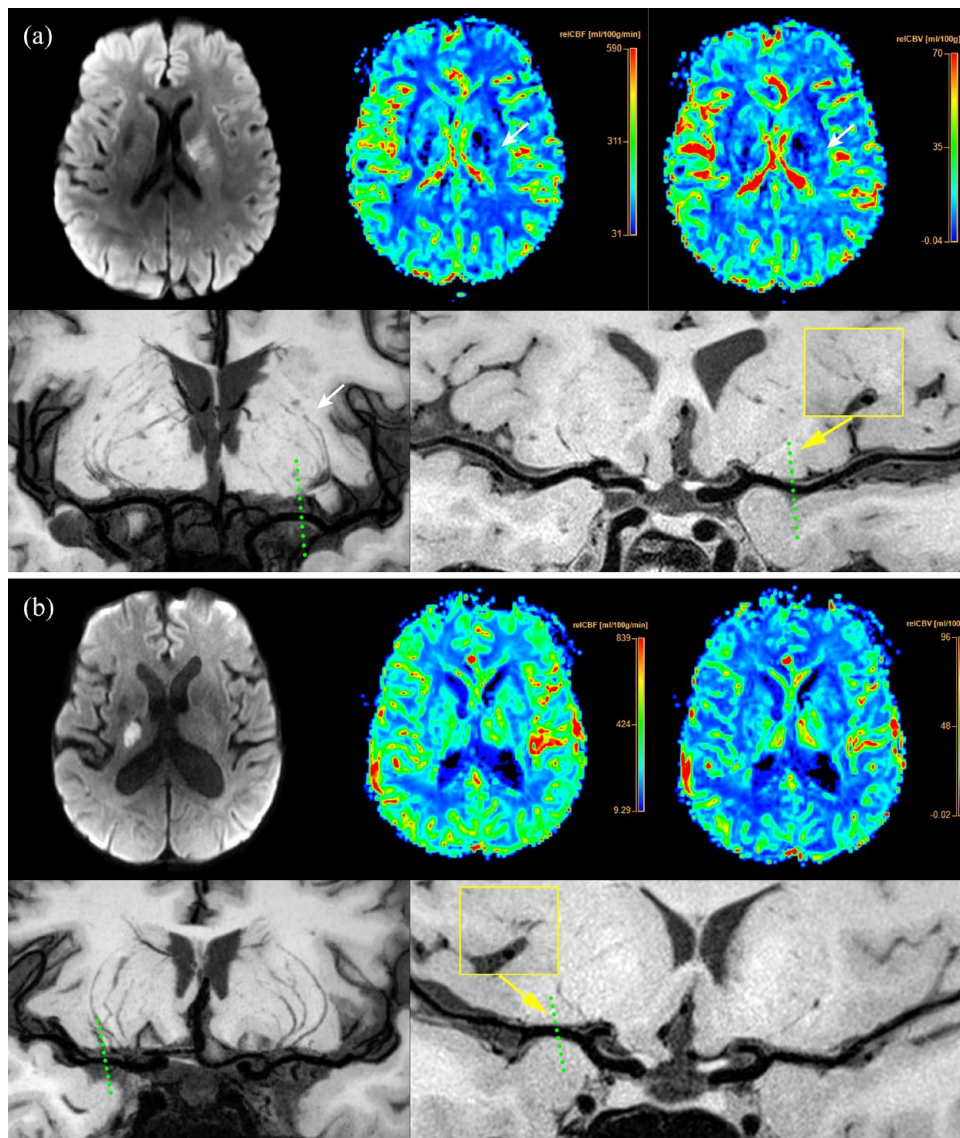


Figure 3. Classification of the etiological subtypes of acute single subcortical infarctions (SSIs). (a) Branch atheromatous disease (BAD) with acute SSIs in the left basal ganglia with reduced cerebral blood flow (CBF) and cerebral blood volume (CBV). Coronal minimum-intensity projection (MinIP) revealed pruning of the left lenticulostriate arteries (LSAs) (white arrow) compared with the right side. Curved multi-planar reconstruction (MPR) of vessel-wall imaging (VWI) showed a culprit plaque adjacent to the corresponding LSA origins (dashed lines), demonstrated by the magnified image on cross-section view (yellow frame). (b) Lacunar infarction related to cerebral small vessel disease (CSVD-related LI) with acute SSIs in the right basal ganglia with normal CBF and CBV. Coronal MinIP revealed almost symmetrical LSAs in the right and left sides. Curved MPR showed no culprit plaque on the relevant carrier artery (dashed lines), demonstrated by the magnified image on cross-section view (yellow frame).

variables were presented as mean \pm standard deviation (SD) or median [interquartile range (IQR)]. Differences in continuous variables between the two groups were assessed using Student's *t* test in the case of normally distributed data, or the Mann–Whitney *U* test in the case of skewed data. Differences in categorical variables

were assessed using chi-square or Fisher's exact test. Multivariable logistic regression was used to adjust factors that might confound the calculation of perfusion parameters for the two subtypes of SSIs, BAD or CSVD-related LI. Differences associated with $p < 0.05$ were considered statistically significant.

Table 1. Baseline demographic, clinical, and perfusion parameters of acute SSI patients.

Characteristics	N = 110
Demographics	
Male, n (%)	87 (79.1)
Age, years (mean ± SD)	54.76 ± 10.26
Risk factors, n (%)	
Hypertension	63 (57.3)
Diabetes	31 (28.2)
Hyperlipidemia	31 (28.2)
Current smoking	62 (56.4)
Body mass index, kg/m ² (mean ± SD)	25.00 ± 3.18
Clinical data	
SBP at admission, mmHg (mean ± SD)	149.52 ± 21.34
DBP at admission, mmHg (mean ± SD)	92.06 ± 14.49
Baseline NIHSS, median (IQR)	3 (2–6)
3-month mRS, median (IQR)	1 (1–2)
3-month mRS ≥ 2, n (%)	48 (43.6)
END, n (%)	30 (27.3)
BAD, n (%)	78 (70.9)
Onset to MRI time, day, median (IQR)	5 (3–7)
Perfusion parameters	
rCBF, median (IQR)	1.00 (0.82–1.14)
rCBV, median (IQR)	0.98 (0.87–1.22)
rMTT, median (IQR)	1.05 (0.96–1.13)
rTTP, median (IQR)	1.00 (1.00–1.02)

Values are n (%), mean ± SD or median (interquartile range). BAD, branch atheromatous disease; DBP, diastolic blood pressure; END, early neurological deterioration; IQR: interquartile range; mRS, modified Rankin Scale; NIHSS, National Institutes of Health Stroke Scale; rCBF, relative cerebral blood flow; rCBV, relative cerebral blood volume; rMTT, relative mean transit time; rTTP, relative time to peak; SBP, systolic blood pressure; SD, standard deviation; SSI, single subcortical infarction.

Results

Patient characteristics

A total of 170 patients were prospectively registered in the acute SSIs database of West China Hospital, of whom 60 were excluded due to

infarction in the brainstem ($n=18$), lack of diffusion restriction lesions on DWI ($n=14$), poor image quality ($n=7$), middle cerebral artery stenosis ($n=4$), evidence of other causes ($n=2$), incomplete MRI sequence ($n=9$), or lack of MRI examination within 7 days of symptom onset ($n=6$). The final analysis included 110 patients with SSIs (Table 1), of whom 87 (79.1%) were male. Mean age of patients was 54.76 ± 10.26 years, and median NIHSS at baseline was 3 (IQR 2–6). The median 3-month mRS was 1 (IQR 1–2), and 48 patients (43.6%) had 3-month mRS ≥ 2 . END was observed in 30 patients (27.3%), and 78 patients (70.9%) were diagnosed with BAD. Median time from the onset of symptoms to MRI scan was 5 days (IQR 3–7).

Correlation between perfusion patterns and LSA characteristics

Based on PWI, 22 of the 110 patients (20%) had hypoperfusion (≥ 1 abnormal perfusion parameter) at the site of the DWI lesion, while the remaining 88 patients (80%) showed normal perfusion (Figure 2). The baseline demographic characteristics, vascular risk factors, stroke severity, functional outcome, and infarct dimensions were similar between the two groups (Table 2). However, incidence of END [10/22 (45.5%) versus 20/88 (22.7%); $p=0.032$] and BAD [20/22 (90.9%) versus 58/88 (65.9%); $p=0.021$] was significantly higher in patients with hypoperfusion than in those with normal perfusion. The hypoperfusion group was also associated with shorter average LSA length (23.48 ± 4.81 mm versus 25.47 ± 3.74 mm, $p=0.037$), but the two groups showed no significant differences in the average LSA distance or tortuosity, numbers of stems and branches, or the median time between symptom onset and MRI scan (Table 2).

Correlation of SSI subtypes with perfusion parameters, LSA characteristics, and clinical profiles

Based on VWI, 78 patients (70.9%) were diagnosed with BAD and 32 (29.1%) with CSVD-related LI (Figure 3). Patients with BAD had significantly lower rCBF [0.95 (IQR 0.81–1.12) versus 1.04 (IQR 0.92–1.22); $p=0.022$] and rCBV [0.95 (IQR 0.84–1.15) versus 1.14 (IQR 0.97–1.27); $p=0.007$] than patients with CSVD-related LI, but no significant differences were observed for rMTT or rTTP (Table 3). After

Table 2. Baseline demographic, clinical profiles, and LSA characteristics of the two perfusion patterns.

Characteristics	Hypoperfusion (<i>n</i> = 22)	Normal perfusion (<i>n</i> = 88)	<i>p</i> value
Demographics			
Male, <i>n</i> (%)	19 (86.4)	68 (77.3)	0.558
Age, years (mean ± SD)	53.36 ± 12.82	55.11 ± 9.58	0.477
Risk factors, <i>n</i> (%)			
Hypertension	13 (59.1)	50 (56.8)	0.847
Diabetes	9 (40.9)	22 (25.0)	0.138
Hyperlipidemia	5 (22.7)	26 (29.5)	0.525
Current smoking	10 (45.5)	52 (59.1)	0.249
Body mass index, kg/m ² (mean ± SD)	24.74 ± 3.16	25.07 ± 3.20	0.675
Clinical data			
SBP at admission, mmHg (mean ± SD)	151.00 ± 27.16	149.15 ± 19.78	0.718
DBP at admission, mmHg (mean ± SD)	89.82 ± 17.59	92.62 ± 13.66	0.420
Baseline NIHSS, median (IQR)	3.5 (2–6.25)	3 (2–5.75)	0.723
3-month mRS ≥ 2, <i>n</i> (%)	11 (50.0)	37 (42.0)	0.501
END, <i>n</i> (%)	10 (45.5)	20 (22.7)	0.032
BAD, <i>n</i> (%)	20 (90.9)	58 (65.9)	0.021
Onset to MRI time, day, median (IQR)	6 (4–7)	5 (3–7)	0.120
LSA characteristics			
Number of LSA stems, median (IQR)	5 (3.75–6)	4 (3–5.75)	0.211
Number of LSA branches, median (IQR)	6 (5–9.25)	7 (5–8)	0.706
Average length of LSAs, mm (mean ± SD)	23.48 ± 4.81	25.47 ± 3.74	0.037
Average distance of LSAs mm (mean ± SD)	19.63 ± 3.85	21.04 ± 3.25	0.082
Average tortuosity of LSAs (mean ± SD)	1.21 ± 0.06	1.21 ± 0.07	0.967
Infarct dimensions			
Infarct volume, ml, median (IQR)	1.44 (0.94–3.42)	1.65 (0.78–3.06)	0.687
Axial lesion diameter, cm, median (IQR)	1.83 (1.30–2.69)	1.62 (1.19–2.05)	0.192
Values are <i>n</i> (%), mean ± SD or median (interquartile range). BAD, branch atheromatous disease; DBP, diastolic blood pressure; END, early neurological deterioration; IQR, interquartile range; LSA, lenticulostriate artery; mRS, modified Rankin Scale; NIHSS, National Institutes of Health Stroke Scale; SBP, systolic blood pressure; SD, standard deviation.			

adjustment for hypertension, number of LSA branches and infarct volume of SSI in multivariable logistic regression, the association of lower rCBF and rCBV with BAD patients remained

significant (Table 4). In addition, the BAD group showed significantly fewer branches and higher incidences of END and poor functional outcome (3-month mRS ≥ 2), as well as larger infarction

Table 3. Main clinical and radiological data of patients with BAD and CSVD-related LI.

Characteristics	BAD (n = 78)	CSVD-related LI (n = 32)	p value
Demographics			
Male, n (%)	62 (79.5)	25 (78.1)	0.873
Age, years (mean ± SD)	55.79 ± 9.70	52.25 ± 11.28	0.100
Risk factors, n (%)			
Hypertension	49 (62.8)	14 (43.8)	0.066
Diabetes	24 (30.8)	7 (21.9)	0.346
Hyperlipidemia	25 (32.1)	6 (18.8)	0.159
Current smoking	43 (55.1)	19 (59.4)	0.683
Body mass index, kg/m ² (mean ± SD)	25.04 ± 3.00	24.91 ± 3.64	0.848
Perfusion parameters			
rCBF, median (IQR)	0.95 (0.81-1.12)	1.04 (0.92-1.22)	0.022
rCBV, median (IQR)	0.95 (0.84-1.15)	1.14 (0.97-1.27)	0.007
rMTT, median (IQR)	1.05 (0.96-1.14)	1.06 (0.96-1.13)	0.989
rTTP, median (IQR)	1.00 (1.00-1.03)	1.00 (0.99-1.02)	0.353
LSA characteristics			
Number of LSA stems, median (IQR)	4 (3-5)	5 (4-6)	0.137
Number of LSA branches, median (IQR)	6 (4-8)	7 (6-9)	0.024
Average length of LSAs, mm (mean ± SD)	25.11 ± 4.31	24.98 ± 3.32	0.877
Average distance of LSAs, mm (mean ± SD)	20.84 ± 3.54	20.55 ± 3.08	0.683
Average tortuosity of LSAs (mean ± SD)	1.21 ± 0.06	1.21 ± 0.07	0.767
Clinical data			
Baseline NIHSS, median (IQR)	4 (2-6)	2.5 (1-4.75)	0.093
3-month mRS ≥ 2, n (%)	39 (50.0)	9 (28.1)	0.036
END, n (%)	26 (33.3)	4 (12.5)	0.026
Onset to MRI time, day, median (IQR)	5 (3-7)	5 (3-7)	0.535
Infarct dimensions			
Infarct volume, ml, median (IQR)	1.99 (0.99-3.40)	1.05 (0.69-2.14)	0.020
Axial lesion diameter, median (IQR)	1.70 (1.34-2.16)	1.53 (1.15-1.96)	0.121

Values are n (%), mean ± SD or median (interquartile range).

BAD, branch atheromatous disease; CSVD-related LI, lacunar infarction related to cerebral small vessel disease; END, early neurological deterioration; IQR: interquartile range; LSAs, lenticulostriate arteries; mRS, modified Rankin Scale; NIHSS, National Institutes of Health Stroke Scale; rCBF, relative cerebral blood flow; rCBV, relative cerebral blood volume; rMTT, relative mean transit time; rTTP, relative time to peak; SD, standard deviation.

volume than patients with CSVD-related LI. However, the two groups did not differ significantly in baseline demographics, risk factors, or NIHSS scores. For details, see Tables 3 and 4.

Discussion

In this study, we prospectively recruited patients with SSIs who underwent combined magnetic resonance PWI and VWI within 7 days of stroke onset and found that compromised cerebral perfusion was associated with impairments in the LSA territory and could be detected by PWI even several days after the onset of symptoms. In addition, our results also showed that the underlying etiology of SSIs may influence the perfusion alterations. Perfusion abnormalities were more prevalent in SSI patients with BAD and were significantly associated with the occurrence of END. To our knowledge, our study would appear to be the first to assess the potential utility of PWI and VWI in investigating the association of perfusion status with LSA morphology and SSI pathogenesis.

Few studies have used computed tomography (CT) or MRI to track changes in cerebral perfusion in patients with SSIs. Due to the dynamic nature of cerebral perfusion, most studies have observed SSIs mainly within 24h of symptom onset and have reported perfusion deficits ranging from 52.2% to 76%.^{4-6,8,18-20} Anecdotally, a sustained perfusion abnormality for more than 24h has been reported in patients with strokes of various etiologies, mostly strokes affecting large vessels.²¹⁻²³ For instance, investigation of the ischemic stroke etiology of different DWI/PWI patterns revealed a mismatch in 19% of acute stroke patients who underwent MRI at 72h after the symptom onset.²¹ Another study of patients with acute stroke across a broad time range reported that almost 25% of patients had mismatch at 24–48 h, and one patient showed mismatch even at 52h after stroke.²² Consistent with these results, we detected perfusion abnormalities in the subacute phase of patients with SSIs within 7 days of the onset of stroke symptoms, while the two perfusion groups showed no significant difference in the interval between symptom onset and perfusion imaging.

Our study showed that hypoperfusion is associated with shorter average LSA length, suggesting that cerebral perfusion alterations might play an

Table 4. Multivariable analysis for perfusion parameters associated with subtypes of SSIs.^a

Variables	OR (95% CI)	p value ^b
rCBF	0.979 (0.959–0.999)	0.036
rCBV	0.980 (0.963–0.997)	0.020
rMTT	0.627 (0.044–8.880)	0.730
rTTP	0.813 (0.136–4.848)	0.820

CI, confidence interval; OR, odds ratio; rCBF, relative cerebral blood flow; rCBV, relative cerebral blood volume; rMTT, relative mean transit time; rTTP, relative time to peak; SSIs, single subcortical infarctions.

^aBranch atheromatous disease (BAD) was compared with lacunar infarction related to cerebral small vessel disease (CSVD-related LI).

^bData were adjusted for hypertension, number of LSA branches, and infarct volume using binary logistic regression analysis.

important role in LSA impairment.²⁴ Various pathological changes in penetrating arteries can reduce blood flow in the small arterioles and thereby reduce LSA patency in VWI images.²⁵ In addition, hemodynamic insufficiency was also found to be related to the occurrence of END in SSIs. This finding is consistent with a previous study reporting that a higher MTT ratio (>1.26) and a lower CBF ratio (<0.76) in perfusion CT scans can predict progressive lacunar infarction in the LSA territory.²⁶ Nevertheless, our results support that minor perfusion defects cannot efficiently predict poor functional outcomes at 3 months, in line with earlier findings.^{8,19,22} It is possible that a longer time from the onset of symptoms to PWI scans could be associated with a higher frequency of recanalization,^{6,23,27} and consequently, the minor hypoperfusion might not indicate that tissue is at risk. However, it remains unclear whether this minor perfusion disturbance in SSIs could be a contributor to long-term post-stroke cognitive impairment or the occurrence of neuroimaging markers of CSVD. Longitudinal investigation of cerebral perfusion alteration in SSIs is warranted to validate this hypothesis.

Our etiological classification of SSI subtypes based on VWI suggests that CBF and CBV abnormalities are more frequent among patients with BAD than those with CSVD-related LI, suggesting that hemodynamics play an important role in the pathogenesis of BAD. A recent perfusion MRI study showed that BAD patients were

associated with fewer normal perfusion patterns, but BAD in that study was diagnosed based only on infarct sites on conventional brain MRI.⁴ BAD involving persistent perfusion defects has been attributed to atherothrombotic blockage of penetrating arteries with less autoregulation, or to insufficient collateral blood flow from adjacent vascular territories, which is often concomitant with larger lesion size.^{2,28,29} We also showed that patients with BAD were more prone to END and had a worse 3-month functional outcome, consistent with previous studies.^{30,31} This may be partly explained by the larger infarct size in BAD patients.³² However, previous studies including our own have suggested that it was the underlying pathogenesis rather than the size of the lesion that determined the END or prognosis in patients with SSI.^{33,34}

It is possible to interpret our data as supporting a link between perfusion change and CSVD-related LI, which would support Fisher's 'lacunar hypothesis'.^{1,2} However, this hypothesis remains controversial,^{35,36} with several studies suggesting that perfusion alteration does not play a significant role in the development of CSVD-related LI.⁹ For example, radiological studies in patients and animal models suggest that the pathogenesis of CSVD-related LI is more likely due to endothelial dysfunction or blood-brain barrier leakage than to arteriolar occlusion.^{35,37-39} Our study was designed to explore not the lacunar hypothesis, but BAD pathogenesis in SSIs, so future work should explore the mechanisms behind CSVD-related LI.

Here, we found no significant differences between the two subtypes in average LSA length or distance, probably due to the partial recanalization of previously occluded perforators in BAD or to the adequate collateral circulation between proximal anastomoses of LSAs in delayed imaging. Thus, we expect that PWI during the subacute stage of SSIs may help distinguish BAD from pure lacunar infarction.

Such differential diagnosis may be important for optimizing the treatment of patients with SSIs, since most patients are admitted after the hyperacute stroke window. The infarction of SSIs may spread beyond the initially hypoperfused area over several days, mainly as a result of altered hemodynamics and cytotoxicity after the initial ischemic insult.^{10,40} Thus, efforts to inhibit spread of ischemic damage may benefit patients in the

subacute phase of SSIs, especially those with BAD. Future work should also examine optimal strategies for preventing secondary stroke in SSI patients and for exploring PWI and hemodynamic disturbances as a way to monitor response to therapy or to predict prognosis, which may be better than methods based on traditional imaging modalities.

Our study had also some limitations. First, we used a definition of hypoperfusion of SSIs that was not based on validated perfusion parameter thresholds, which reflects the lack of relevant data.¹⁵ We used the relatively sensitive threshold of 25% perfusion reduction to ensure detection of PWI lesion during the subacute stage of SSIs. Larger studies should be performed to determine exact thresholds for distinguishing hypoperfused tissues in SSIs. In contrast, our aim in the present study was to explore the relationship between potential hemodynamic changes and the etiology of SSIs. Second, since perfusion changes over time after stroke, investigating SSIs with a single PWI scan may mask the complexity of the underlying pathophysiology. Hence, longitudinal investigation of SSI patients is needed to clarify the association of minor hemodynamic changes with the heterogeneous pathogenesis and, potentially, long-term cognitive impairment. Third, the ROI that we defined may not have included the peripheral area with less severely impaired perfusion, because diffusion and perfusion images were co-registered to acquire small perfusion defects only within the DWI lesion. However, since PWI lesions usually regress during the subacute stage, this may not have substantially affected the accuracy of perfusion measurements.

In conclusion, our study demonstrates that PWI can provide important insights into the pathophysiology of acute SSIs. We also showed that compromised cerebral perfusion is related to LSA impairments and the occurrence of BAD in SSIs. Nevertheless, additional studies are needed to determine the clinical significance of perfusion abnormalities in acute SSIs and their potential role as therapeutic targets.

Ethics approval and consent to participate

The study was approved by the Ethics Committee of West China Hospital (2018521) and was conducted according to the principles of the Declaration of Helsinki. All subjects provided written informed consent before enrollment.

Consent for publication

Not applicable.

Author contributions

Shuai Jiang: Conceptualization; Data curation; Formal analysis; Investigation; Software; Visualization; Writing – original draft.

Jing-Yu Cui: Formal analysis; Methodology; Software; Visualization.


Yu-Ying Yan: Investigation; Methodology; Resources.

Tang Yang: Investigation; Methodology.

Wen-Dan Tao: Resources; Supervision.

Bo Wu: Conceptualization; Project administration; Resources; Supervision; Validation; Writing – review & editing.

ORCID iD

Shuai Jiang  <https://orcid.org/0000-0003-2140-1535>

Acknowledgements

We thank Marc Fisher (Department of Neurology, Beth Israel Deaconess Medical Center and Harvard Medical School, Boston, MA, USA) for his constructive suggestions on the manuscript. We also thank Jie Liu (ICAP, Philips Healthcare, Chengdu, China) for his contribution to image analysis.

Funding

The authors disclosed receipt of the following financial support for the research, authorship, and/or publication of this article: This work was supported by the National Natural Science Foundation of China (81870937 and 82071320), the 1·3·5 Project for Disciplines of Excellence–Clinical Research Incubation Project of West China Hospital at Sichuan University (2020HXFH012), and the 1·3·5 Project for Disciplines of Excellence of West China Hospital at Sichuan University (ZYG D18009).

Conflict of interest statement

The authors declared no potential conflicts of interest with respect to the research, authorship, and/or publication of this article.

Availability of data and materials

Data are available upon reasonable request from the corresponding author.

References

1. Fisher CM. Lacunes: small, deep cerebral infarcts. *Neurology* 1965; 15: 774–784.
2. Fisher CM. The arterial lesions underlying lacunes. *Acta Neuropathol* 1968; 12: 1–15.
3. Caplan LR. Intracranial branch atheromatous disease: a neglected, understudied, and underused concept. *Neurology* 1989; 39: 1246–1250.
4. Huang YC, Lee JD, Pan YT, *et al.* Perfusion defects and collateral flow patterns in acute small subcortical infarction: a 4D dynamic MRI study. *Transl Stroke Res* 2021; 13: 399–409.
5. Forster A, Kerl HU, Wenz H, *et al.* Diffusion- and perfusion-weighted imaging in acute lacunar infarction: is there a mismatch. *PLoS ONE* 2013; 8: e77428.
6. Förster A, Mürle B, Böhme J, *et al.* Perfusion-weighted imaging and dynamic 4D angiograms for the estimation of collateral blood flow in lacunar infarction. *J Cereb Blood Flow Metab* 2016; 36: 1744–1754.
7. Campbell BC, Christensen S, Tress BM, *et al.* Failure of collateral blood flow is associated with infarct growth in ischemic stroke. *J Cereb Blood Flow Metab* 2013; 33: 1168–1172.
8. Poppe AY, Coutts SB, Kosior J, *et al.* Normal magnetic resonance perfusion-weighted imaging in lacunar infarcts predicts a low risk of early deterioration. *Cerebrovasc Dis* 2009; 28: 151–156.
9. Gerraty RP, Parsons MW, Barber PA, *et al.* Examining the lacunar hypothesis with diffusion and perfusion magnetic resonance imaging. *Stroke* 2002; 33: 2019–2024.
10. Doege CA, Kerskens CM, Romero BI, *et al.* Assessment of diffusion and perfusion deficits in patients with small subcortical ischemia. *AJNR Am J Neuroradiol* 2003; 24: 1355–1363.
11. Zhang Z, Fan Z, Kong Q, *et al.* Visualization of the lenticulostriate arteries at 3T using black-blood T1-weighted intracranial vessel wall imaging: comparison with 7T TOF-MRA. *Eur Radiol* 2019; 29: 1452–1459.
12. Jiang S, Yan Y, Yang T, *et al.* Plaque distribution correlates with morphology of lenticulostriate arteries in single subcortical infarctions. *Stroke* 2020; 51: 2801–2809.
13. Jiang S, Cao T, Yan Y, *et al.* Lenticulostriate artery combined with neuroimaging markers of cerebral small vessel disease differentiate the pathogenesis of recent subcortical infarction. *J Cereb Blood Flow Metab* 2021; 41: 2105–2115.

14. Hong L, Ling Y, Su Y, *et al.* Hemispheric cerebral blood flow predicts outcome in acute small subcortical infarcts. *J Cereb Blood Flow Metab* 2021; 41: 2534–2545.
15. Bandera E, Botteri M, Minelli C, *et al.* Cerebral blood flow threshold of ischemic penumbra and infarct core in acute ischemic stroke: a systematic review. *Stroke* 2006; 37: 1334–1339.
16. Tatu L, Moulin T, Bogousslavsky J, *et al.* Arterial territories of the human brain: cerebral hemispheres. *Neurology* 1998; 50: 1699–1708.
17. Kim BJ, Lee DH, Kang DW, *et al.* Branching patterns determine the size of single subcortical infarctions. *Stroke* 2014; 45: 1485–1487.
18. Huang YC, Tsai YH, Lee JD, *et al.* Hemodynamic factors may play a critical role in neurological deterioration occurring within 72 hrs after lacunar stroke. *PLoS ONE* 2014; 9: e108395.
19. Rudilosso S, Laredo C, Mancosu M, *et al.* Cerebral perfusion and compensatory blood supply in patients with recent small subcortical infarcts. *J Cereb Blood Flow Metab* 2019; 39: 1326–1335.
20. Das T, Settecase F, Boulos M, *et al.* Multimodal CT provides improved performance for lacunar infarct detection. *AJNR Am J Neuroradiol* 2015; 36: 1069–1075.
21. Restrepo L, Jacobs MA, Barker PB, *et al.* Etiology of perfusion-diffusion magnetic resonance imaging mismatch patterns. *J Neuroimaging* 2005; 15: 254–260.
22. Kane I, Hand PJ, Rivers C, *et al.* A practical assessment of magnetic resonance diffusion-perfusion mismatch in acute stroke: observer variation and outcome. *J Neurol* 2009; 256: 1832–1838.
23. Barber PA, Darby DG, Desmond PM, *et al.* Prediction of stroke outcome with echoplanar perfusion- and diffusion-weighted MRI. *Neurology* 1998; 51: 418–426.
24. Chen YC, Wei XE, Lu J, *et al.* Correlation between the number of lenticulostriate arteries and imaging of cerebral small vessel disease. *Front Neurol* 2019; 10: 882.
25. Kang CK, Park CA, Park CW, *et al.* Lenticulostriate arteries in chronic stroke patients visualised by 7 T magnetic resonance angiography. *Int J Stroke* 2010; 5: 374–380.
26. Yamada M, Yoshimura S, Kaku Y, *et al.* Prediction of neurologic deterioration in patients with lacunar infarction in the territory of the lenticulostriate artery using perfusion CT. *Am J Neuroradiol* 2004; 25: 402–408.
27. Suzuki T, Natori T, Sasaki M, *et al.* Evaluating recanalization of relevant lenticulostriate arteries in acute ischemic stroke using high-resolution MRA at 7T. *Int J Stroke: Off J Int Stroke Soc* 2020; 16: 1093–1046.
28. Mohr JP. Lacunes. *Stroke* 1982; 13: 3–11.
29. Caplan LR. Lacunar infarction and small vessel disease: pathology and pathophysiology. *J Stroke* 2015; 17: 2–6.
30. Yamamoto Y, Ohara T, Hamanaka M, *et al.* Characteristics of intracranial branch atheromatous disease and its association with progressive motor deficits. *J Neurol Sci* 2011; 304: 78–82.
31. Jeong HG, Kim BJ, Yang MH, *et al.* Neuroimaging markers for early neurologic deterioration in single small subcortical infarction. *Stroke* 2015; 46: 687–691.
32. Shinohara Y, Kato A, Kuya K, *et al.* Perfusion MR imaging using a 3D pulsed continuous arterial spin-labeling method for acute cerebral infarction classified as branch atheromatous disease involving the lenticulostriate artery territory. *Am J Neuroradiol* 2017; 38: 1550–1554.
33. Yan Y, Jiang S, Yang T, *et al.* Lenticulostriate artery length and middle cerebral artery plaque as predictors of early neurological deterioration in single subcortical infarction. *Int J Stroke*. Epub ahead of print 17 March 2022. DOI: 10.1177/17474930221081639.
34. Zhang C, Wang Y, Zhao X, *et al.* Distal single subcortical infarction had a better clinical outcome compared with proximal single subcortical infarction. *Stroke* 2014; 45: 2613–2619.
35. Wardlaw JM, Dennis MS, Warlow CP, *et al.* Imaging appearance of the symptomatic perforating artery in patients with lacunar infarction: occlusion or other vascular pathology? *Ann Neurol* 2001; 50: 208–215.
36. Pantoni L. Cerebral small vessel disease: from pathogenesis and clinical characteristics to therapeutic challenges. *Lancet Neurol* 2010; 9: 689–701.
37. Wardlaw JM, Smith C and Dichgans M. Small vessel disease: mechanisms and clinical implications. *Lancet Neurol* 2019; 18: 684–696.

38. Cuadrado-Godia E, Dwivedi P, Sharma S, *et al.* Cerebral small vessel disease: a review focusing on pathophysiology, biomarkers, and machine learning strategies. *J Stroke* 2018; 20: 302–320.
39. Jiang S, Wu S, Zhang S, *et al.* Advances in understanding the pathogenesis of lacunar stroke: from pathology and pathophysiology to neuroimaging. *Cerebrovasc Dis* 2021; 50: 588–596.
40. Fiebach JB, Hopt A, Vucic T, *et al.* Inverse mismatch and lesion growth in small subcortical ischaemic stroke. *Eur Radiol* 2010; 20: 2983–2989.

Visit SAGE journals online
[journals.sagepub.com/
home/tan](https://journals.sagepub.com/home/tan)

 SAGE journals